Characterization of the Heat Extraction Capability of a Compliant, Sliding, Thermal Interface for Use in a High Temperature, Vacuum, Microgravity Furnace

Jenny Bellomy-Ezell
Sverdrup Technologies Inc., Huntsville, AL

Jeff Farmer
NASA Marshall Space Flight Center

Shawn Breeding, Reggie Spivey
TecMasters Inc., Huntsville, AL

ABSTRACT
A compliant, thermal interface material is tested to evaluate its thermal behavior at elevated temperatures, in vacuum conditions, and under varying levels of compression. Preliminary results indicate that the thermal performance of this polymer fiber-based, felt-like material is sufficient to meet thermal extraction requirements for the Quench Module Insert, a Bridgman furnace for microgravity material science investigation. This paper discusses testing and modeling approaches employed, gives of a status of characterization activities and provides preliminary test results.

Introduction

A common type of furnace used in Microgravity material science investigations is a Bridgman furnace consisting of hot zone for melting a long, thin, cylindrical sample (typically a metal alloy), and a cold zone for extracting heat from the sample to resolidify it. The primary function of this configuration is to induce a large temperature gradient along the length of the sample at approximately the location of the interface of the solid and liquid regions of the sample. Additionally, this furnace translates relative to the sample such that the translation rate of the furnace is equal to the rate at which the solid liquid interface moves (this corresponds to the solidification rate). An example of this type of furnace, currently being developed, is the Quench Module Insert (QMI), [Ref]. The QMI furnace will be installed as part of the Microgravity Science Research Facility (MSRF); one of the first science facilities planned to fly aboard the International Space Station (ISS).

In the current QMI design, the cold zone consists of the water-cooled outer section surrounding a conical shaped insert. On the inner diameter of this insert is a felt or velvet-like material that serves as the primary thermal interface with the sample assembly.

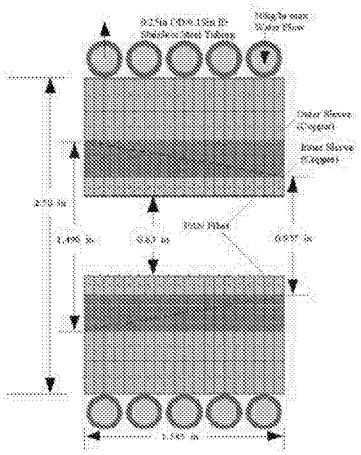

Figure 1. Schematic of Replaceable Cold Zone.

This felt is composed of carbon polymer fibers, which are perpendicularly attached to a substrate, which is then affixed to the replaceable cold zone insert. This material is a product called Vel-Therm and is produced by a

company in California called Energy Sciences Lab, Inc. This velvet-like material is both compliant, allowing the material to brush against the sample assembly surface during translation, and highly thermally conductive, providing for high heat extraction rates by the cold zone. These high heat extraction rates, in turn produce high sample thermal gradients required by the scientific investigations (>100 °C/cm for some QMI investigations) that will use this furnace.

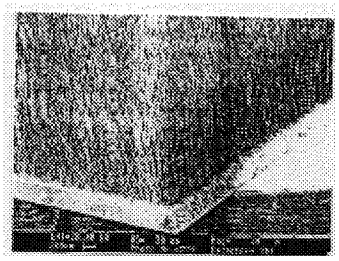

Figure 2. Isometric View of Oriented Fibers and Substrate Comprising the Vel-Therm felt.

This conductive couple is particularly important for QMI due to the vacuum environment in which it operates. Without this conductive couple, heat would have to be extracted from the sample via only radiation across the vacuum gap between the cold zone and sample assembly. At the temperatures required for the investigations using QMI, this would severely limit the heat extraction and consequently the attainable sample thermal gradients.

The Vel-Therm material was developed via a Small Business Innovative Research Contract, [ref]. In this early development work the thermal performance of the material was characterized in an air environment at low temperatures. In addition, since that early investigation the vendor, ESLI, has made substantial improvements in the material. Consequently, additional testing was required to characterize the thermal behavior of the new material and to do so in conditions resembling those of QMI, namely higher temperature and vacuum. The data derived from this activity is to be used to evaluate the material's performance sensitivity to various QMI design parameters and to provide quantitative data for use in the QMI thermal models. In addition, the data will be used to help select the appropriate Vel-Therm and set proper operating limits. This paper outlines the approach and results of this characterization.

Test Matrix

The test results of two different Vel-Therm types are presented in this paper. In designing the test setup, parameters were selected to simulate the actual furnace specifications as closely as possible. For example, the temperature the felt would be exposed to ranged from 100 to 600 °C in the furnace. Therefore, the setpoint temperatures bound this range. Also, for each felt tested, we wanted to examine different initial gap size settings. These gap settings were typically based on a percentage of felt height, which is the sum of fiber length, thickness of substrate and thickness of the adhesive.

Table 1. Vel-Therm Characterization Test Matrix

Felt Type	**Set Point Temp (°C)**	**Gap Size (mils)**	**Gap Size as % of felt height**
J80G	100 - 600	95, 55	99, 40
J120G	100 - 600	120, 114	99, 95

Test Objectives and Approach

The main focus of this test is to measure the heat extraction rate of the Vel-Therm felt as specified by the effective heat transfer coefficient. This effective heat transfer coefficient, h_{eff}, is defined by the following equation:

$$heff = Q / A(T_{Hot} - T_{Cold})$$

Where Q is the heat extracted by cold zone through the felt interface; A is the area of the felt interface; T_{Hot} and T_{Cold} are the temperatures of the hot and cold surfaces, respectively, being coupled via the felt. More importantly, T_{hot} simulates the temperatures seen by the sample assembly and T_{cold} simulates the chill block temperatures.

The primary means of establishing the power being conducted through the felt was to measure the energy transferred to the water passing through the cold side assembly. Consequently, the effective heat transfer in terms of the measured parameters is given in the following equation.

$$heff = \frac{\dot{m}Cp(T_{out} - T_{in})}{A(T_{Hot} - T_{Cold})}$$

Where $\dot{m}$ and Cp are the mass flow rate and the specific heat, respectively, of the cooling water. T_{out} and T_{in} are the outlet and inlet temperatures of the cooling water. A is the surface area over which the Vel-Therm felt is applied. T_{Hot} is the average temperature of the hot (or heated) surface and T_{Cold} is the average temperature of the cold (or cooled) surface. This assumes that the heat lost to the surroundings, either through conduction or radiation, from the cold surface is negligible. It was assumed, and confirmed via analysis, that each surface was approximately isothermal under the specific test conditions.

Test Fixture

Again, we wanted to measure the temperature delta across the water as our means of characterizing the heat transfer performance of the Vel-Therm. Therefore, the test fixture was designed to measure the heat transferred from the top surface of the hot side assembly, to the bottom surface of the chill block, which is actively cooled by a helical fluid loop just under the surface. Both the hot side assembly and the chill block are made of copper. The hot side assembly temperature was targeted to represent those typical of QMI sample assembly and the chill block was controlled to temperatures typical of the QMI cold zone. The two surfaces are coupled with the Vel-Therm, which is bonded to the chill block surface. The gap between the Hot Side Assembly and the Cold Side Assembly was positioned by a scissor-supported plate, which supports the Cold Side Assembly from above.

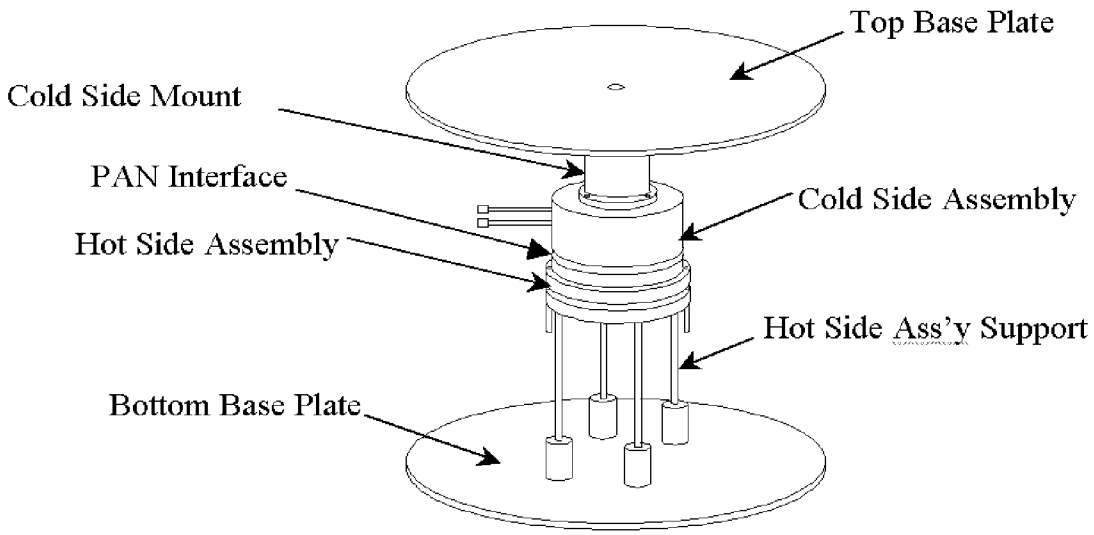

Figure 3. Isometric View of VEL-THERM Test Setup (not to scale)

We also wanted to minimize heat transfer to the chill block in areas other than the Vel-Therm interface. Therefore, to reduce heat loss from the bottom and sides of the Hot Side Assembly, a 6-layer molybdenum radiation shield was constructed around the circumference of the Hot Side Assembly. Additionally, the mating

surfaces of the chill block and hot copper were highly polished in order to minimize radiative coupling between the two surfaces. Furthermore, aluminized tape was adhered to the chill block's circumference to help prevent radiative gains in the chill block thereby further reducing inaccuracies in measured heat load.

Lastly, appropriate instrumentation was applied and the whole assembly was housed in a bell jar and vacuum conditions (P<10-4mbar) imposed. Temperatures of the test assembly were monitored by twelve Type K thermocouples. RTD's were used to measure the water inlets and outlet temperatures.

Thermal Model

While some initial thermal analysis was performed via spreadsheet based hand calculations, the bulk detailed analysis is being performed using PATRAN and P3Thermal. P3Thermal is a geometry-based thermal analysis tool that uses PATRAN as the geometry modeler and mesh generator. P3Thermal accommodates conductive, radiative, and convective transfer in solids and also provides capabilities to assess advective heating of the coolant flow. Details of the PATRAN and P3Thermal are provided in reference 7. The geometric model of the test apparatus is depicted in Figure 4. The molybdenum shields are not shown so that the hot and cold copper assemblies may be viewed.

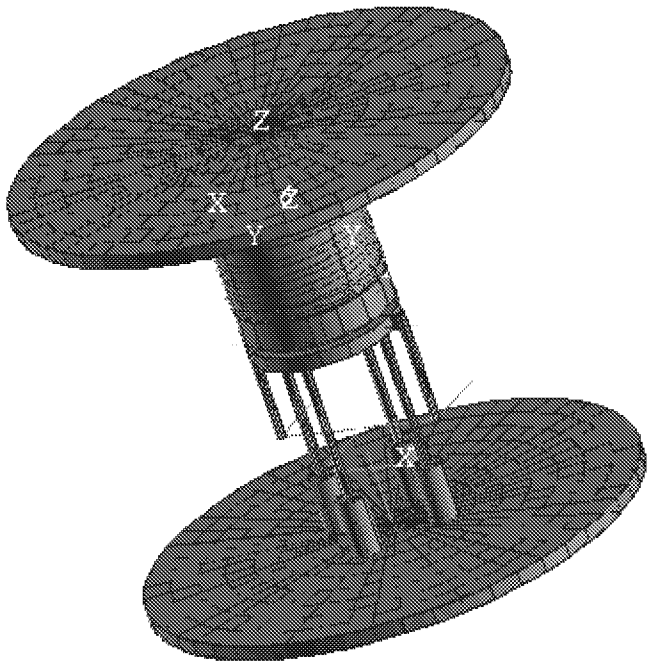

Figure 4. Isometric View of 3D Test Apparatus Test PATRAN/P3THERMAL Model without Radiation Shields.

A number of boundary conditions were applied to the model to simulate the important heat flow paths and thermal sinks. Using P3Thermal, we were able to use multiple enclosures to capture the radiative exchange and heat loss. The area where the VEL-THERM felt is adhered to the chill block and in contact with the heated copper has a convection between regions boundary condition imposed. To accurately simulate the heat transfer to the chill block's helical fluid loop an advective boundary condition was imposed.

The main focus of this on-going analysis is to predict the heater power levels and losses, water cooling rates and temperatures at key locations throughout the test apparatus. This model was also used to validate the isothermality of the chill block area where the Vel-Therm is applied.

Results and Error Assessment

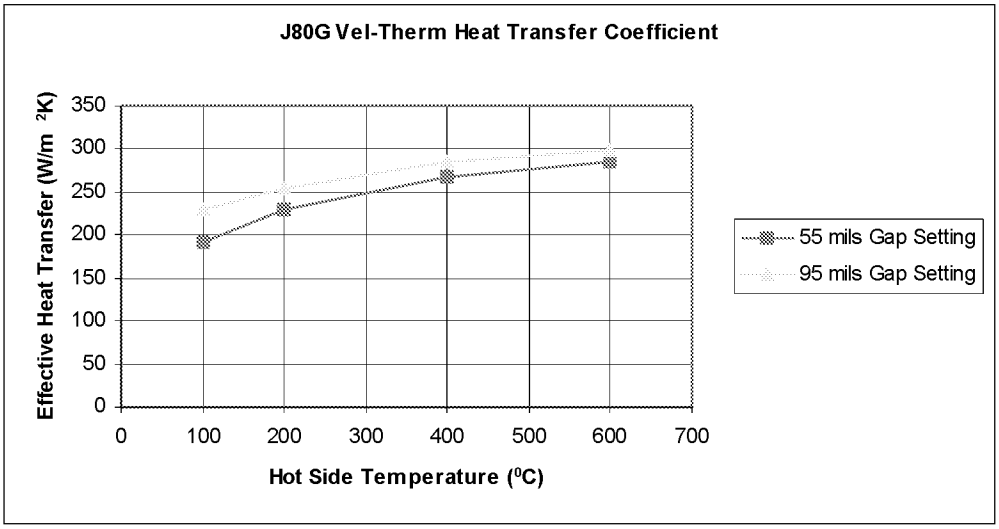

Figure 5. J80G VEL-THERM Heat Transfer Coefficient vs. Hot Side Surface Temperature

The data for the J80G is presented as a function of the hot side temperature and initial gap size. Data was recorded at four temperatures, ranging from 100 to 600°C. The cold surface temperature was maintained between 35 and 40°C. In the first run (55 mil gap size), the fibers are bent to conform to a gap size that is almost half of the fibers' length. It was supposed that increasing the compression could theoretically result in an increase in effective heat transfer coefficient. As the gap shrinks relative to the fiber length, more of the fiber is bent over. The result would be increased surface contact between the fiber the hot side surface and possibly increased contact pressure due to bending the fibers. This increased area and pressure could increase contact conductance. Results for the 55 mil gap size case, however, were actually lower than the second run which had a larger gap size, indicating that h might actually increase with an increasing gap size. The 55 mil gap could have been excessive, damaging some of the fibers.
The gap size for the second run was set to 95 mils such that the fibers were in contact with the hot copper but not bent to the naked eye. Both cases show significant dependence on temperature. This fact could have arisen from increased radiation at elevated hot surface temperatures.

The following sets of curves summarize the results obtained for the second VEL-THERM type tested, the J120G.
Figure 6. J80G VEL-THERM Heat Transfer Coefficient vs. Hot Side Surface Temperature

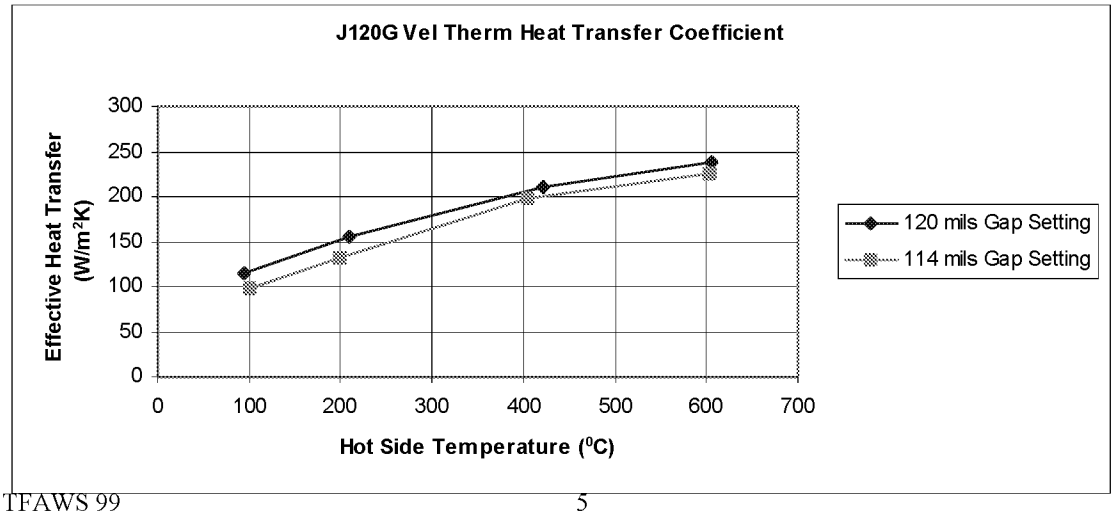

Now, we can see that the data indeed shows a trend indicating that the effective heat transfer coefficient increases as gap size increases. It is not intuitive why this is happening and further testing is needed to investigate this trend. Again, the results indicate temperature dependence. Comparing the different Vel-Therm types, the J80G's performance is superior.

Error Assessment

To provide an error assessment, the heat transfer measured across the water was compared to the heat provided by the power supply. Attempts were made to quantify the heat loss from the heater that occurred in places other than the felt interface. The only significant conduction heat paths were those from the heater leads and the Hot Side Support Structure. Hand calculations were done to quantify the heat loss in this area.

The J80Gf at 600 °C run was chosen for comparison as a worst case scenario. Comparing the wattage from the power supply to the q into the water, the heater power was 119 W higher. The heat transfer down the two heater leads accounted for 27 W. The heat transfer down the four support rods accounted for another 30W.

The only significant radiation heat transfer was that emitted by the Hot Side Assembly. The test setup configuration employs molybdenum radiation shields to insulate the Hot Side Assembly. In addition, the copper block encasing the heater element was polished reducing the emissivity and the radiative losses further. Radiation from the hot copper, support rods and shields was calculated using the equation for infinite concentric

$$q_{12} = \frac{\sigma A_1 (T_1^4 - T_2^4)}{[1/\varepsilon_1 + 1 - \varepsilon_2/\varepsilon_2](r_1/r_2)}$$

cylinders. This identified another 19 W of heat loss.

The heater leads were encapsulated with insulation to exclude interference with the base plate. This insulation provided a heat leak that accounts for 6W. Another possible source of heat loss is into the copper tubing that connects the fluid loop to the flexible tubing of the water pump. Also, radiation from the exposed portions of the surfaces of the copper cylinder where the VEL-THERM is applied may contribute. This accounted for approximately 5 W. This still leaves approximately 30 watts unaccounted for. A possible explanation may be error associated with the measurement devices, either measuring the water flow or the heater output. The unidentified heat loss is less than 10% of the calculated heat transfer into the water. This error may relate to the curve discussed earlier which indicates that heff actually increases as gap size increases. This issue is under investigation.

In addition to the hand calculations, the modeling effort is on going to investigate this heat loss. The test setup is well instrumented, therefore, we are looking at temperatures at various locations to find where the energy loss is occurring. Insights gained from this error assessment will aid in a redesign of the test setup.

Conclusions

Overall, the performance J80G VEL-THERM was in performance, as it had been in the room environment testing. Also, significant temperature dependence was observed in both Vel-Therm types. The results do seem to suggest that the effective heat transfer coefficient increases as gap size increases. Therefore, lower compression rates would be recommended. This trend is not fully understood and will be investigated further. One benefit of utilizing lower compression rates is decreasing the possibility of damaging the fibers. Another benefit of using the lower compression rates is avoiding the misalignment problems caused between the interior surface of the furnace bore and the exterior surface of the SACA during the high processing temperatures when material properties change and expansion occurs.

A possible explanation of the surprising results is the lack of fiber density control. The fiber packing fraction would impact performance by affecting the amount of contact area provided. If it varies from one batch to another more than slightly, the ability to repeat earlier performance is lost. This raises the question of how to control or test each batch before accepting it into inventory. This is an important area of concern and will require future work to resolve.

A great deal of work remains to be done to characterize the heat extraction capability of VelTherm. Namely, resolving the energy balance problem and possibly redesigning the test fixture. Also, examination of the trend indicating that h increases with gap size, since this is not intuitive.

ACKNOWLEDGEMENTS
The author(s) wish to acknowledge the contributions of Phillip Bryant, Kevin Burks, Myscha Crouch and Doug Westra of the Marshall Space Flight Center.

REFERENCES
Quench Module Insert Preliminary Design Review Thermal Design Data Book, NASA-MSFC, TecMaster Inc., Sverdrup Tech., Huntsville, Al, March 1999
Fundamentals of Heat and Mass Transfer, Second Edition, Frank P. Incropera & David P. DeWitt, Purdue University, 1985
Thermophysical Properties of High Temperature Solid Materials, Vol. 1: Elements, Purdue University, The MacMillan ComVel-Thermy, New York
Introduction to Thermal Analysis Using MSC/THERMAL, PAT312, Exercise Workbook, Release 7.5, April, 1998
Satellite Thermal Control Handbook, David G. Gilmore, The Aerospace Corporation Press, El Segundo, California, 1994
Sample Ampoule-Cartridge Assembly For Microgravity Crystal Growth, ESLI, San Diego, CA